AD_____

Award Number: W81XWH-06-1-0196

TITLE: Contrast Agents for Micro-Computed Tomography of Microdamage in Bone

PRINCIPAL INVESTIGATOR: Ryan K. Roeder

CONTRACTING ORGANIZATION: University of Notre Dame
Notre Dame, IN 46556

REPORT DATE: January 2009

TYPE OF REPORT: Annual

PREPARED FOR: U.S. Army Medical Research and Materiel Command
Fort Detrick, Maryland 21702-5012

REPORT DOCUMENTATION PAGE

Form Approved
OMB No. 0704-0188

1. REPORT DATE	2. REPORT TYPE	3. DATES COVERED
1 Jan 2009	Annual	1 Jan 2007 – 31 Dec 2008

4. TITLE AND SUBTITLE

Contrast Agents for Micro-Computed Tomography of Microdamage in Bone

5a. CONTRACT NUMBER

5b. GRANT NUMBER
W81XWH-06-1-0196

5c. PROGRAM ELEMENT NUMBER

6. AUTHOR(S)

Ryan K. Roeder

E-Mail: rroeder@nd.edu

5d. PROJECT NUMBER

5e. TASK NUMBER

5f. WORK UNIT NUMBER

7. PERFORMING ORGANIZATION NAME(S) AND ADDRESS(ES)

University of Notre Dame
Notre Dame, IN 46556

8. PERFORMING ORGANIZATION REPORT NUMBER

9. SPONSORING / MONITORING AGENCY NAME(S) AND ADDRESS(ES)
U.S. Army Medical Research and Materiel Command
Fort Detrick, Maryland 21702-5012

10. SPONSOR/MONITOR'S ACRONYM(S)

11. SPONSOR/MONITOR'S REPORT NUMBER(S)

12. DISTRIBUTION / AVAILABILITY STATEMENT
Approved for Public Release; Distribution Unlimited

13. SUPPLEMENTARY NOTES

14. ABSTRACT

Novel methods have been developed for detecting damaged bone tissue using micro-computed tomography (micro-CT) and contrast agents with higher x-ray attenuation than bone. The ability to non-destructively and three-dimensionally detect the presence, spatial location and accumulation of fatigue microdamage in cortical using micro-CT was demonstrated using a precipitated barium sulfate (BaSO4) stain. Gold nanoparticles (Au NPs) were functionalized with bisphosphonate (alendronate) and carboxylate (L-glutamic acid) ligands, and exhibited stability in physiological solutions, specificity for damaged tissue and a high binding affinity for bone mineral. Synchrotron x-ray tomography was able to detect alendronate and glutamic acid functionalized Au NPs labeling controlled surface damage on cortical bone specimens.

15. SUBJECT TERMS
Bone; Microdamage; Computed Tomography, Contrast Agents; Barium Sulfate; Gold; Nanoparticles

16. SECURITY CLASSIFICATION OF:			17. LIMITATION OF ABSTRACT	18. NUMBER OF PAGES	19a. NAME OF RESPONSIBLE PERSON
a. REPORT	b. ABSTRACT	c. THIS PAGE			19b. TELEPHONE NUMBER *(include area code)*
U	U	U	UU	21	USAMRMC

Table of Contents

Page

INTRODUCTION

Accumulation of microdamage in bone tissue can lead to an increased risk of fracture, including stress fractures in active individuals and fragility fractures in the elderly. Current methods for detecting microdamage are inherently invasive, destructive, tedious and two-dimensional. These limitations inhibit evaluating the effects of microdamage on whole bone strength and prohibit detecting microdamage *in vivo*. Therefore, we are investigating novel methods for detecting microdamage in bone using micro-computed tomography (micro-CT) and contrast agents with higher x-ray attenuation than bone. For proof-of-concept, the presence, spatial variation and accumulation of microdamage in cortical and trabecular bone specimens was nondestructively detected using micro-CT after staining with barium sulfate. However, specimens were stained *in vitro* via a precipitation reaction which was non-specific to damage and not biocompatible. Therefore, we are currently investigating the synthesis and functionalization of gold and barium sulfate nanoparticles for deliverable, damage-specific contrast agents. The objectives of the research are to 1) develop damage-specific contrast agents, with greater x-ray attenuation than bone, for micro-computed tomography (micro-CT) of microdamage; 2) evaluate the x-ray attenuation, deliverability and specificity of contrast agent formulations; and, 3) quantify the effects of the contrast agent on micro-CT images in damaged and undamaged bone, and correlate the measurements to traditional measures of microdamage. Research progress in each of the specific aims is discussed below.

BODY

Task 1: Develop damage-specific contrast agents, with greater x-ray attenuation than bone, for micro-computed tomography (micro-CT) of microdamage (Months 1-24).

Aim 1.1 Synthesize barium sulfate ($BaSO_4$) nanoparticles with a mean size less than 10 nm (Months 1-6).

Completed. $BaSO_4$ nanoparticles and gold nanoparticles (Au NPs) have been synthesized and characterized as described in the January 2008 annual progress report.

Aim 1.2 Stabilize and functionalize colloidal dispersions of $BaSO_4$ nanoparticles with (macro)molecules containing multiple carboxy, hydroxyl and/or phosphonate ligands able to simultaneously bind with both the nanoparticle and calcium ions exposed on surfaces created by microdamage in bone (Months 1-24).

Challenges and new opportunities that were described in the January 2008 annual progress report have been overcome and completed, respectively.

$BaSO_4$ nanoparticles were stabilized by coating with dextran. $BaSO_4$ nanoparticles were prepared using a microemulsion technique as described previously. A third microelmulsion containing soluble dextran and a fourth microemulsion containing epicholorihydrin were added to prepare $BaSO_4$ nanoparticles coated with cross-linked dextran. In contrast to as-synthesized $BaSO_4$ nanoparticles, $BaSO_4$ nanoparticles coated with cross-linked dextran remained stable upon dispersion in water after release from the microemulsion (Fig. 1). The only remaining work within this aim is to functionalize dextran coated $BaSO_4$ nanoparticles with carboxy, hydroxyl and/or phosphonate ligands. This work is in progress and expected to be completed by January 2010.

Au NPs have now been functionalized with carboxylate (reported in January 2009), phosphonate and bisphosphonate groups (Fig. 2). The presence of functional groups was verified by FT-IR (Fig. 3). The particle size (Fig. 4) and the plasmon band for Au NPs in UV-Vis spectroscopy was unchanged after functionalization indicating that the nanoparticles remained dispersed. For additional details, see Ross *et al*. (2009) in the Appendices.

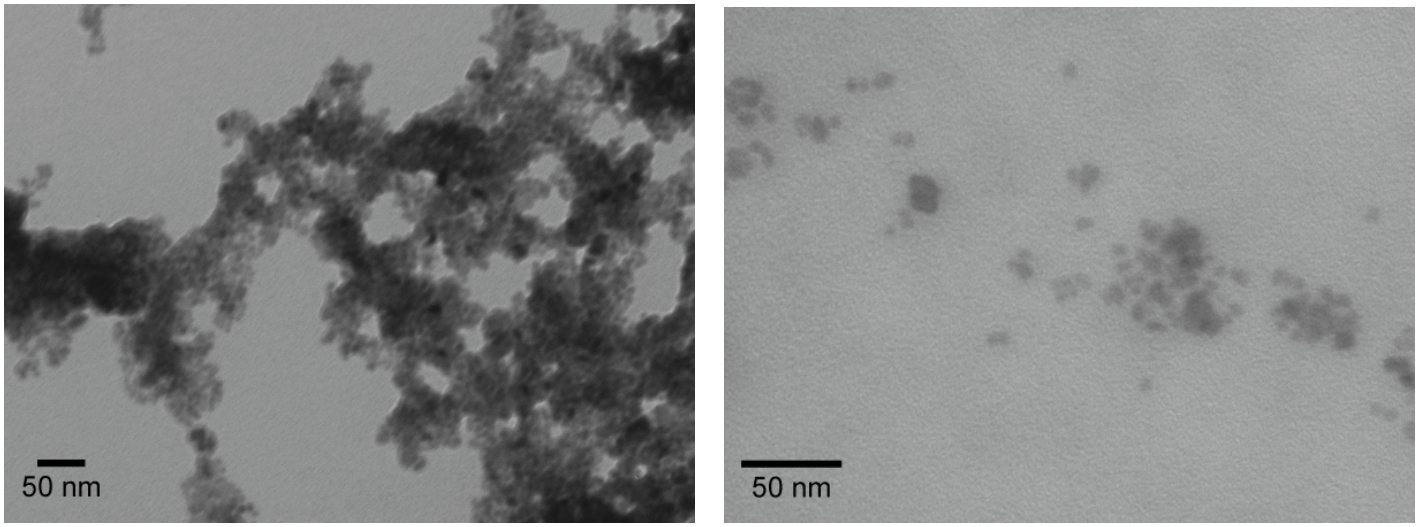

(a) (b)

Fig. 1. Transmission electron micrographs (TEM) micrographs showing (a) agglomerated as-synthesized $BaSO_4$ nanoparticles and (b) dispersed $BaSO_4$ nanoparticles coated with cross-linked dextran after mixing in water upon release from the microemulsion.

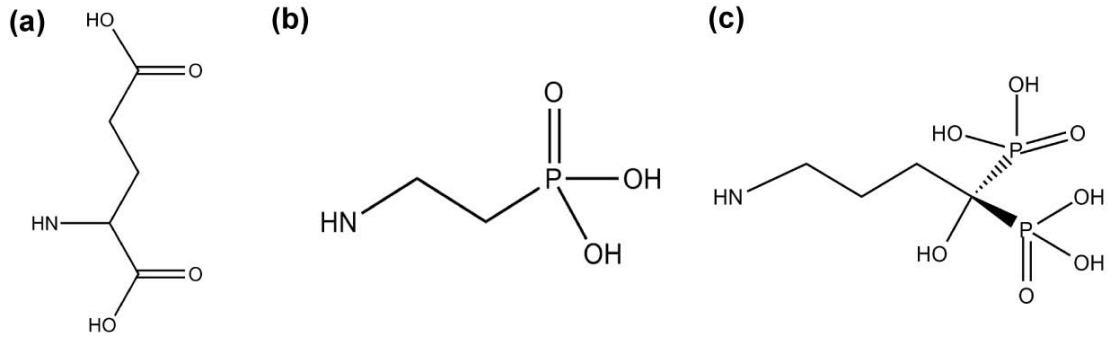

Fig. 2. Au NPs were functionalized with (a) glutamic acid (b) 2-aminoethylphosphonic acid or (c) alendronate. Note that each molecule has amino groups for binding on gold surfaces which are opposite (a) carboxylic acid, (b) phosphonate or (c) bisphosphonate groups for calcium binding damaged tissue.

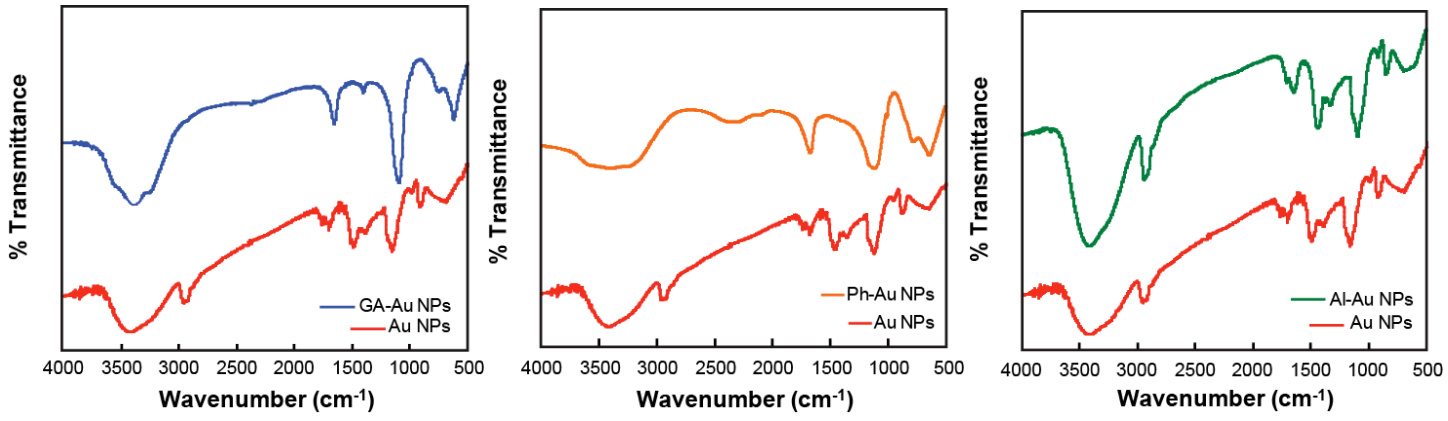

(a) (b) (c)

Fig. 3. FT-IR spectra for Au NPs functionalized with (a) glutamic acid (GA) (b) 2-aminoethylphosphonic acid (Ph) or (c) alendronate (Al), compared with as-synthesized Au NPs.

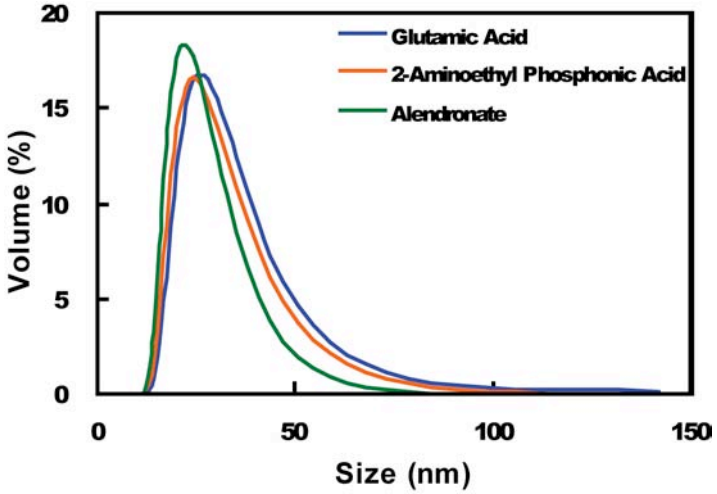

Fig. 4. Particle size distributions of functionalized Au NPs measured by dynamic light scattering (DLS) (Malvern Zetasizer Nano-ZS).

Aim 1.3 Synthesize iodinated molecules containing multiple phosphonate ligands with a high binding affinity for calcium ions exposed on surfaces created by microdamage in bone (Months 1-24).

Completed. For reasons discussed in the January 2008 report, this aim was modified to focus on phosphonate functionalized Au NPs. Results were described in Aim 1.2 above.

Task 2: Evaluate the x-ray attenuation, deliverability and specificity of contrast agent formulations (Months 6-36).

Aim 2.1 Measure the particle size and/or molecular weight of the contrast agent (Months 1-12).

Completed. $BaSO_4$ nanoparticles and Au NPs have been synthesized and characterized as described in the January 2008 annual progress report and above.

Aim 2.2 Measure the mass attenuation and partial volume effect of known concentrations of the contrast agents on micro-CT images (Months 7-18).

A commercial, polychromatic micro-CT scanner (ScanCo μCT-80, ≈10 μm resolution) has not yet been able to detect the Au NPs at the small size and low concentration required for a deliverable contrast agent. Therefore, we explored the detection limit of our scanner using well-defined volumes of gold deposited within a material of similar x-ray attenuation to cortical bone tissue. Photolithography was used to deposit an array of gold islands into acid-etched aluminum (Fig. 5). The array consists of square islands ranging in size from 1 to 100 μm, and deposited to thicknesses of 1 μm, 500 nm and 100 nm. Aluminum is well-known to exhibit similar x-ray attenuation to cortical bone tissue and is thus used for commercial/clinical x-ray phantoms. Specimen edge effects were mitigated by "sandwiching" the gold islands against another polished aluminum surface, such that edge detection is aluminum-gold-aluminum without the presence of air. The polychromatic micro-CT was able to reliably detect 20 x 20 x 1 μm and 30 x 30 x 0.5 μm and larger gold islands, but was not able to detect any islands at 100 nm thickness (Fig. 6).

A proposal for synchrotron x-ray tomography was submitted to the Advanced Photon Source at Argonne National Laboratory and awarded. The full proposal is provided in the Appendices. Twenty-four hours of beam time was used in October 2008 and another twenty-four hours beam time will be used in March 2009. Use of this facility enabled the highest resolution available (≈100 nm) and the x-ray energy to be tailored to maximize the difference in attenuation between bone and gold at the L-edge of gold between 12 and 11.8 keV. Synchrotron x-ray tomography was able to image all the gold islands described above, even at the 100 nm thickness. Three-dimensional reconstructions of these images are being processed. Synchrotron x-ray tomography was also able to detect alendronate and glutamic acid functionalized Au NPs labeling controlled

surface damage on a bovine cortical bone specimens (Fig. 7). While this result is encouraging and we will continue to seek additional beam time, we will only be able to image a small number of specimens limited to at least one cross-section dimension of approximately 1 mm in order to get sufficient transmission at low energies. Thus, we cannot rule out that a possible negative result from this project will be that deliverable, damage-specific contrast agents are not able to be detected in bone tissue using current, commercially available CT imaging technology, and we will continue to investigate labeling of fatigue microdamage using the precipitated $BaSO_4$ stain, as described in Task 3 below.

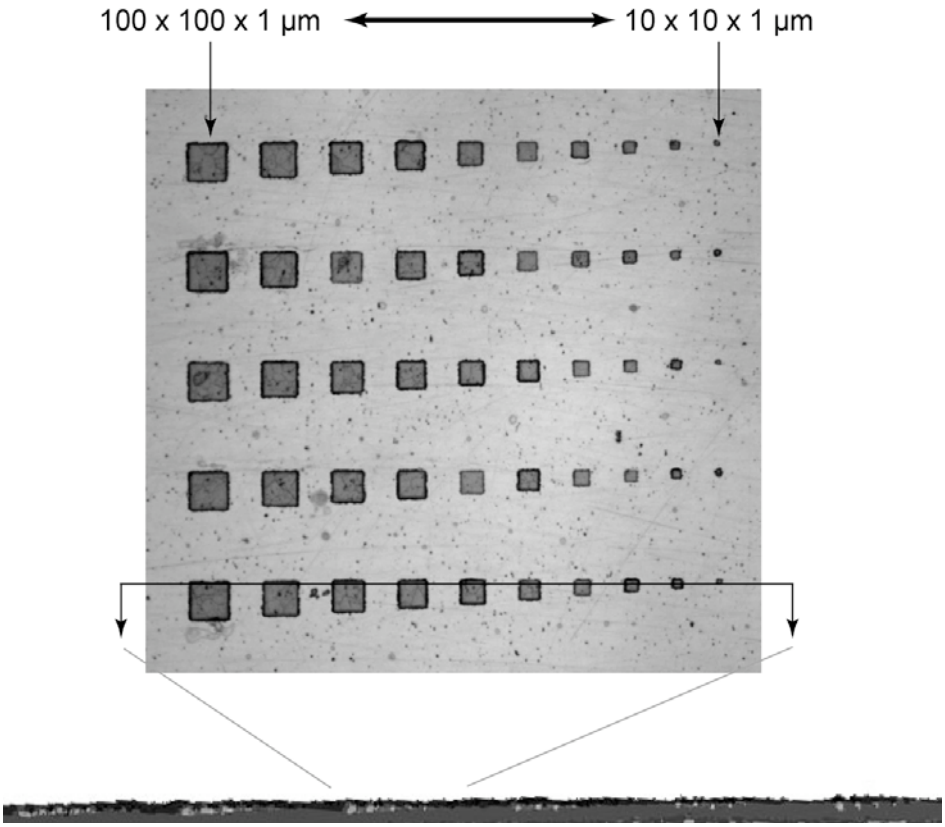

Fig. 5. Optical micrograph (above) showing an array of gold islands (darker) deposited on an aluminum (lighter) substrate and a thresholded micro-CT slice (below) at 10 μm resolution showing the gold islands (brighter) in cross-section on the surface of the aluminum (darker) substrate.

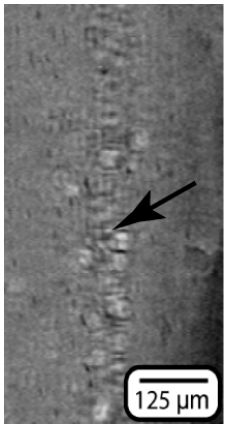

Fig. 7. Synchrotron x-ray tomography slice of bovine cortical bone specimen showing enhanced contrast in the scratched region (labeled by an arrow) corresponding to the presence of alendronate functionalized Au NPs.

(a) (b) (c)

Fig. 6. Reconstructed polychromatic micro-CT images at 10 μm resolution for gold islands deposited to a thickness of (a) 1 μm, (b) 500 nm and (c) 100 nm.

Finally, a new collaboration was formed with Adel Faridani of Oregon State University who is an expert in reconstruction algorithms for x-ray tomography. Several image data sets have been sent for analysis with results pending.

Aim 2.3 Determine the stability of the contrast agent in phosphate buffered saline, simulated body fluid (SBF) and/or fetal bovine serum (FBS) (Months 13-24).

Completed. See results described above under Aim 1.2. Furthermore, conductivity and zeta potential measurements showed evidence for a change from electrostatic to steric stabilization for functionalized Au NPs in both water (Fig. 8) and PBS. The stability of functionalized Au NPs in phosphate buffered saline (PBS) and fetal bovine serum (FBS) was also evident from measurements performed for Aim 2.4 below.

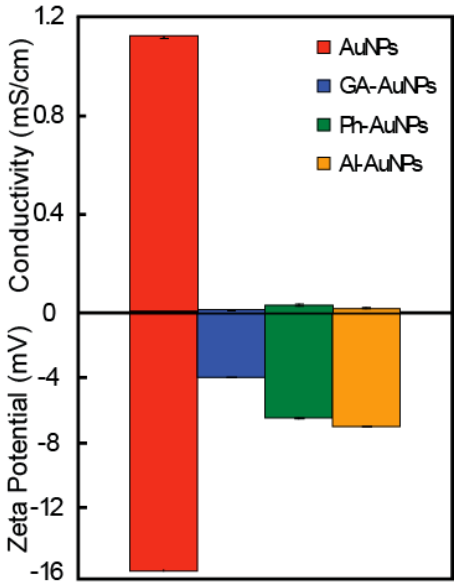

Fig. 8. Conductivity and zeta potential of aqueous dispersions of as-synthesized and glutamic acid (GA), 2-aminoethylphosphonic acid (Ph) and alendronate (Al) functionalized Au NPs.

Aim 2.4 Validate the specificity of the contrast agent for microdamage using machined surfaces of bovine cortical bone (Months 19-30).

The specificity of glutamic acid, 2-aminoethylphosphonic acid and alendronate functionalized Au NPs for damaged tissue was first verified and qualitatively compared using scratched surfaces of bovine cortical bone. Specimens were scratched with a scalpel to induce controlled surface damage and then soaked in a solution of functionalized Au NPs. Specimens were characterized using optical microscopy, backscattered scanning electron microscopy (SEM), energy dispersive X-ray analysis (EDXA) and synchrotron x-ray tomography. Alendronate functionalized Au NPs exhibited the highest specificity, as expected, and consequently provided the most visible staining of damaged tissue in optical microscopy (Fig. 9) and backscattered SEM (Fig. 10). Surface damage on similarly prepared specimens labeled with alendronate and glutamic acid functionalized Au NPs was able to be detected using synchrotron x-ray tomography as described above (Fig. 7).

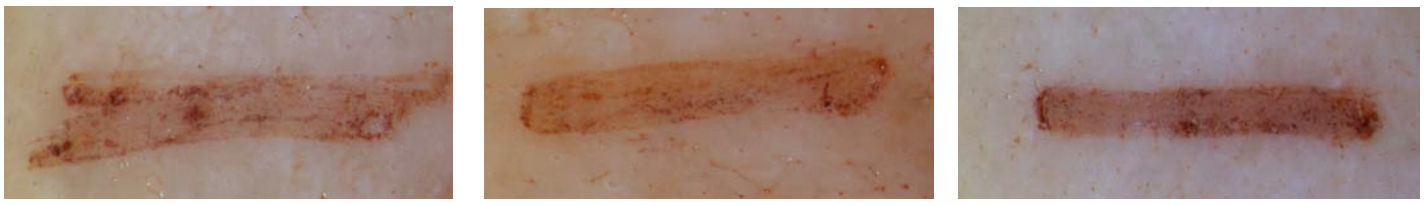

(a) (b) (c)

Fig. 9. Optical micrographs of bovine cortical bone surface damage labeled with (a) glutamic acid, (b) phosphonic acid and (c) alendronate functionalized Au NPs, showing the characteristic red color of Au NPs labeling the scratched surface. Note that the width of the scratch is approximately the same as that in Fig. 10.

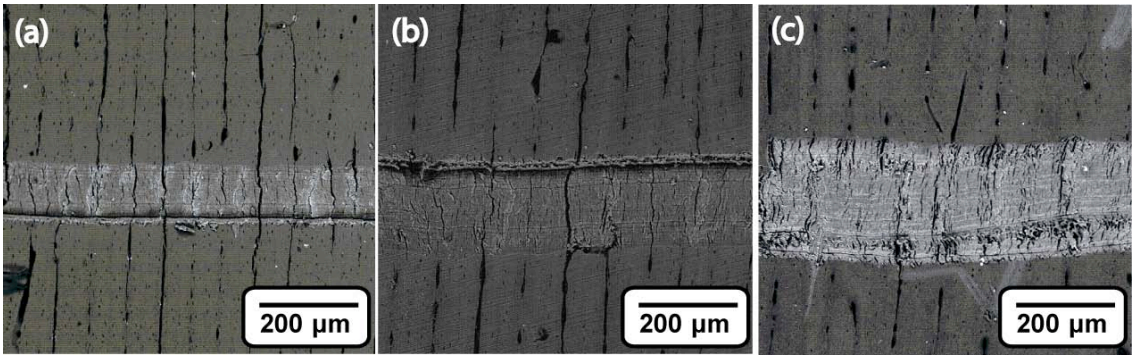

Fig. 10. Backscattered SEM micrographs of bovine cortical bone surface damage (scratch) labeled with (a) glutamic acid, (b) phosphonic acid and (c) alendronate functionalized Au NPs, showing enhanced contrast between damaged and non-damaged tissue correlating to the binding affinity of each functional group.

Quantitative measurements of the binding affinity were performed by adding hydroxyapatite (HA) crystals to functionalized Au NP solutions in DI water. The suspension was incubated for a period of time to allow for binding and centrifuged. Transmission electron microscopy (TEM) was used to verify the presence of Au NPs bound to the surface of the HA crystals (Fig. 11). The supernatant solution was collected and the residual gold concentration was measured using inductively coupled plasma optical emission spectroscopy (ICP-OES). The kinetics of binding with time showed that alendronate functionalized Au NPs were bound much more rapidly, but that all three formulations were nearly 100% bound to the HA crystals after 24 h (Fig. 12). Therefore, subsequent measurements for determining binding constants were taken at 4 h with varying concentration (Fig. 13). Binding saturation was reached at approximately 1.2, 0.5 and 6.0 mg/g for glutamic acid, phosphonic acid and alendronate, respectively. Binding constants were derived using a half-reciprocal linearization of Langmuir isotherms. Binding constants of the functionalized Au NPs were 0.72, 0.25 and 3.82 mg/L for glutamic acid, phosphonic acid and alendronate, respectively, corresponding to a maximum of 1.22, 0.48 and 7.33 mg Au NPs bound per gram of hydroxyapatite. Thus, alendronate functionalized Au NPs exhibited the highest specificity, as expected.

In summary, the binding affinity and imaging contrast of functionalized Au NPs was greatest using alendronate followed by glutamic acid and phosphonic acid. For further experimental details, see Ross *et al*. (2009) in the Appendices. Additional binding experiments have recently been preformed in fetal bovine serum to simulate an *in vivo* environment, and the data is being processed.

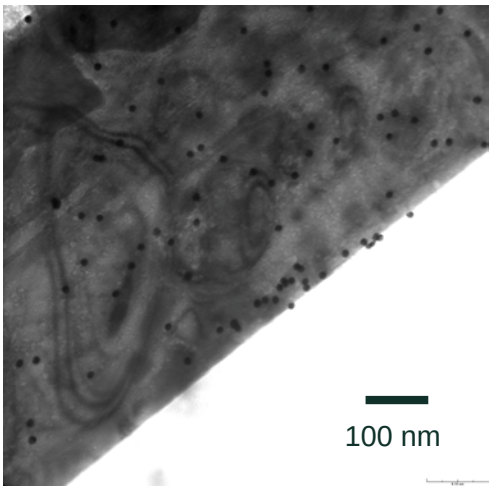

Fig. 11. TEM micrograph showing functionalized Au NPs attached to the surface of an HA crystal.

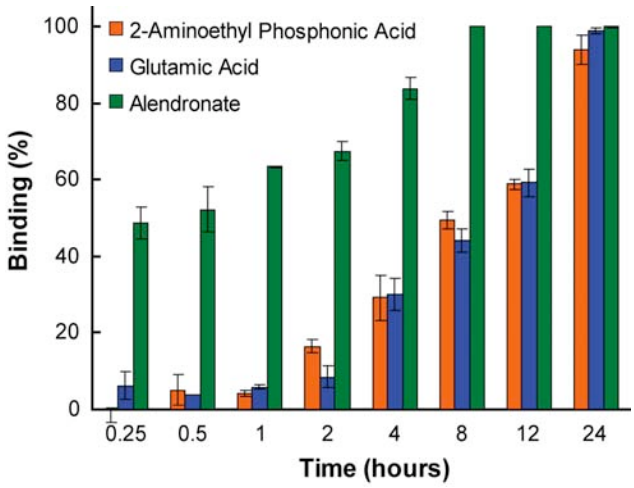

Fig. 12. Kinetics of binding for glutamic acid, phosphonic acid and alendronate functionalized Au NPs to HA crystals in DI water.

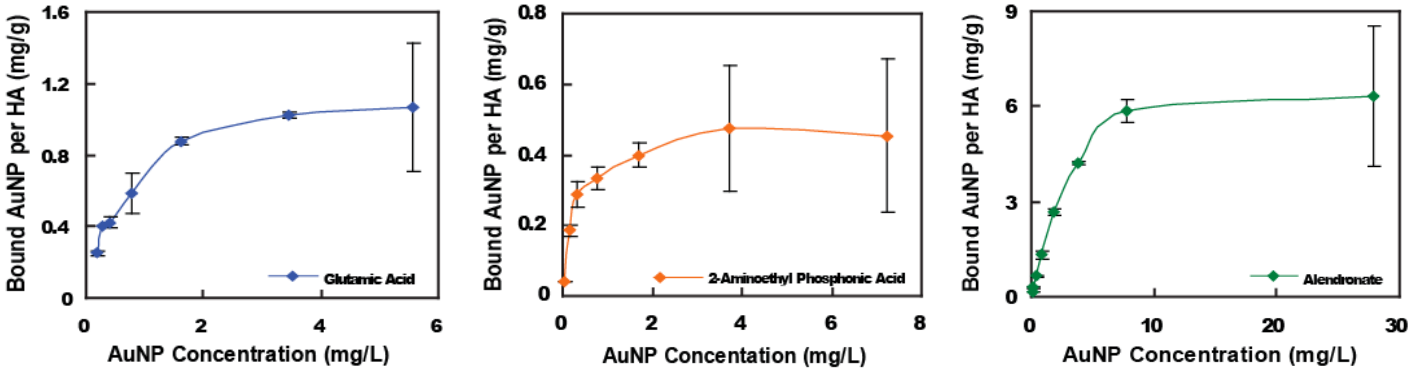

(a) (b) (c)

Fig. 13. Binding affinity of (a) glutamic acid, (b) phosphonic acid and (c) alendronate functionalized Au NPs to HA crystals after 4 h in DI water. Binding constants were derived from this data using a half-reciprocal linearization of Langmuir isotherms.

Aim 2.5 Measure the diffusivity of the contrast agent into both cortical and trabecular bone tissue (Months 25-36).

The January 2008 annual progress report described the preparation of Au NPs were conjugated with fluoroscein in order to most easily track the diffusion of Au NPs in bone tissue using epifluorescence. Experiments showed specificity for damage and that the contrast agent readily diffused into cortical bone tissue. However, quantitative measurements of diffusivity were inhibited by difficulty correlating levels of fluorescence to gold concentration. An experimental apparatus for using bone tissue specimens as a membrane separating a functionalized Au NP solution from DI water (or PBS) was constructed and will be used this spring to measure the diffusivity from the concentration of gold in the solutions with time using ICP-OES.

Task 3: Quantify the effects of the contrast agent on micro-CT images in damaged and undamaged bone, and correlate the measurements to traditional measures of microdamage (Months 25-48).

Due to the present requirement that our deliverable, damage-specific contrast agents (functionalized Au NPs) be imaged using synchrotron x-ray tomography, experiments for Task 3 have moved forward with a precipitated $BaSO_4$ stain. While this stain is not damage-specific nor biocompatible (e.g., suited for *ex vivo* studies only), it is able to be imaged using a commercially available polychromatic micro-CT and has been demonstrated to detect fatigue microdamage [1,2]. Validation studies using this technique will enable nondestructive, three-dimensional imaging of microdamage by micro-CT, which would provide a useful new methods for the scientific study of microdamage in bone.

Aim 3.1 Quantify the measured mass attenuation in rectangular notched and un-notched human cortical bone bending specimens, and correlate micro-CT measurements to the microdamage density measured by fluorescent staining and microscopy (Months 25-42).

We originally proposed to conduct these experiments using four-point bending fatigue. However, experiments in our lab have demonstrated a number of inherent problems in the use of four-point bending for the study of fatigue microdamage in cortical bone [3]. Therefore, we have used cyclic uniaxial tension to detect the presence and location of fatigue microdamage and/or propagating cracks within human cortical bone using micro-CT with a precipitated $BaSO_4$ contrast agent. Non-specific $BaSO_4$ staining was observed on the free surface and scattered within some Haversian canals in unloaded control specimens (Figs. 14 and 15). All specimens loaded in cyclic uniaxial tension also exhibited at least one distinct region of concentrated $BaSO_4$ stain which appeared characteristic of fatigue damage and/or propagating cracks (Figs. 14 and 15). The ratio of the thresholded $BaSO_4$ stain volume to bone volume (SV/BV) increased from the unloaded control group to specimens loaded to a 5 and 10% loss in elastic modulus ($p < 0.05$, *t*-test) (Fig. 16). Thus, micro-CT was able

to detect a relatively small volume and small differences in the amount of fatigue microdamage within a uniformly stressed volume of human cortical bone using a $BaSO_4$ contrast agent. Note that the micro-CT scanner (10 μm resolution) could not detect this damage without the use of a contrast agent. For additional details, see Landrigan *et al*. (2009) in the Appendices.

Additional specimens from the above study were mechanically loaded using an identical protocol, blinded and sent to Dr. David Burr's histology lab at the Indiana University Medical Center for staining with basic fuchsin and histomorphometry. We expect their measurements to be completed this spring, providing a blinded, independent validation of our micro-CT methods.

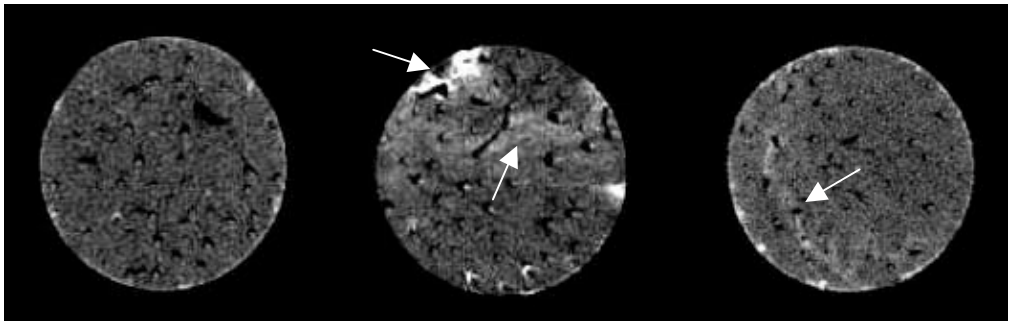

(a) (b) (c)

Fig. 14. Specimen cross-sections (2.5 mm diameter) imaged by micro-CT showing (a) non-specific $BaSO_4$ staining (bright voxels) in unloaded control specimens, and (b,c) regions of concentrated $BaSO_4$ staining in specimens loaded in cyclic uniaxial tension. Arrows highlight regions of $BaSO_4$ staining characteristic of fatigue damage and/or propagating microcracks.

Fig. 15. Three-dimensional micro-CT reconstructions of the entire gauge section (2.5 mm diameter) in a (left) unloaded control specimen and (right) specimen loaded in cyclic uniaxial tension. Arrows highlight regions of $BaSO_4$ staining characteristic of fatigue damage and/or propagating microcracks.

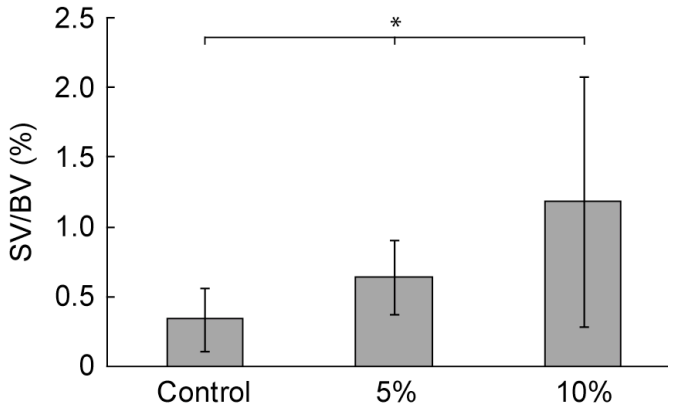

Fig. 16. The ratio of $BaSO_4$ stain volume to total bone volume (SV/BV) in thresholded micro-CT images was significantly greater for the loaded specimens compared to the unloaded control group, and between groups loaded to 5 and 10% modulus degradation. Asterisks denote statistically significant differences ($p < 0.05$, *t*-test). Error bars show one standard deviation.

Aim 3.2 Quantify locations and levels of microdamage in trabecular bone subjected to torsional loading, and validate the measurements by comparing to fluorescent staining and microscopy (Months 37-48).

Preliminary results to have shown that in undamaged samples the non-specific $BaSO_4$ staining does not alter the x-ray signal in comparison to samples that were not treated with the contrast agents. Staining and post-

staining protocols were investigated to determine the best approach to eliminate false positive results. The primary determinant is effective clearing of the precipitates from the pore space using a water jet. Samples are presently being prepared for the torsional loading study. Two groups of samples will be studied and stained with either aqueous barium chloride and sodium sulfate or emulsions. The mechanical testing is expected to be completed in the first half of 2009.

Aim 3.3 Quantify microdamage in whole rat femurs subjected to bending (Months 37-48).

We expect to obtain rat femora from our animal facility and begin this experiment in the summer of 2009.

Timeline

Progress toward the above Tasks and Aims is on schedule, given a six month window from the official award date (1/1/06) until the time key personnel (e.g., the postdoc and GAs) were in place. A request for a six month extension is possible during the final project year.

KEY RESEARCH ACCOMPLISHMENTS (last year)

- Barium sulfate ($BaSO_4$) nanoparticles were stabilized by coating with cross-linked dextran.
- Gold nanoparticles (Au NPs) were functionalized with bisphosphonate (alendronate) and carboxylate (L-glutamic acid) ligands, and exhibited stability in physiological solutions, specificity for damaged tissue and a high binding affinity for bone mineral.
- Synchrotron x-ray tomography was able to detect alendronate and glutamic acid functionalized Au NPs labeling controlled surface damage on cortical bone specimens.
- The ability to non-destructively and three-dimensionally detect the presence, spatial location and accumulation of fatigue microdamage in cortical using micro-CT was demonstrated using a precipitated $BaSO_4$ stain.

REPORTABLE OUTCOMES

Journal Publications

H. Leng, X. Wang, R.D. Ross, G.L. Niebur and R.K. Roeder, “Micro-computed tomography of fatigue microdamage in cortical bone using a barium sulfate contrast agent,” *J. Mech. Behav. Biomed. Mater.*, **1** [1] 68-75 (2008).

Conference Proceedings and Abstracts

R.D. Ross and R.K. Roeder, “Functionalized Gold Nanoparticle X-ray Contrast Agents for Bone Tissue,” *Trans. of the 35th Annual Meeting of the Society for Biomaterials*, San Antonio, TX, **32**, (2009).

M.D. Landrigan, G.L. Niebur and R.K. Roeder, “Detection of Fatigue Microdamage in Human Cortical Bone Using Micro-Computed Tomography,” *Trans. of the 55th Annual Meeting of the Orthopaedic Research Society*, Las Vegas, NV, **34**, 2143 (2009).

M.D. Landrigan and R.K. Roeder, “Comparison of Measures of Mechanical Degradation During Four-Point Bending Fatigue of Cortical Bone,” *Trans. of the 55th Annual Meeting of the Orthopaedic Research Society*, Las Vegas, NV, **34**, 322 (2009).

M.D. Landrigan, H. Leng, R.D. Ross, C. Berasi, X. Wang, G.L. Niebur and R.K. Roeder, “Imaging Microdamage in Bone Using a Barium Sulfate Contrast Agent,” *2009 TMS Annual Meeting*, San Francisco, CA (2009).

R.D. Ross and R.K. Roeder, “Molecular Surface Modification of Gold Nanoparticles to Impart Specificity to Damaged Bone Tissue,” *2009 TMS Annual Meeting*, San Francisco, CA (2009).

R.D. Ross, Z. Zhang and R.K. Roeder, "Functionalized Gold Nanoparticles as an X-ray Contrast Agent for Bone Microdamage," *2008 TMS Annual Meeting*, New Orleans, LA (2008). **1st place in the Graduate Division of the Biological Materials Science Symposium Student Poster Contest. NSF Travel Award Recipient.**

Personnel Report (including new degrees and employment)

Name	Role	Period	% Effort	New Degrees	Current Position
Ryan K. Roeder	PI	1/06-	8	n/a	promoted to Assoc. Prof. with tenure
Glen L. Niebur	co-PI	1/06-	8	n/a	promoted to Assoc. Prof. with tenure
Zhenyuan Zhang	Postdoc	6/06-12/07	100	n/a	Research Scientist, Sandia Nat. Lab.
Huijie Leng	GA	1/06-10/06	100	PhD (2006)	Assoc. Prof., Peking Univ. Third Hosp.
Matt Landrigan	GA	6/06-	100	MS (2007)	pursuing PhD at Notre Dame
Ryan Ross	GA	8/06-	100		pursuing PhD at Notre Dame
Jackie Garrison	GA	1/08-	100		pursuing PhD at Notre Dame
Matt Meagher	UG RA	6/06-8/06	100	BS (2008)	unknown
Paul Baranay	UG RA	6/07-8/07	100		pursuing BS at MIT
Carl Berasi	UG RA	1/07-	unpaid		pursuing BS at Notre Dame
Erin Heck	UG RA	1/07-5/07	unpaid		pursuing BS at Notre Dame
Jimmy Buffi	UG RA	8/07-5/08	unpaid	BS (2008)	pursuing PhD at Northwestern
Bridget Leone	UG RA	1/08-	unpaid		pursuing BS at Notre Dame

Note that GA = graduate assistant and UG RA = undergraduate research assistant.

Research Opportunities Received

GUP10463, three shifts in Station 13-BMD, GSECARS, Advanced Photon Source, Argonne National Laboratory, October 9-10, 2008.

GUP10463, three shifts in Station 13-BMD, GSECARS, Advanced Photon Source, Argonne National Laboratory, February 27-28, 2009.

CONCLUSION

A biocompatible, deliverable, damage-specific contrast agent with greater x-ray attenuation than bone would enable non-destructive, three-dimensional and non-invasive (*in vivo*) imaging of microdamage in bone. Such a contrast agent would have the potential to enable clinical assessment of bone quality and damage accumulation, and scientific study of damage processes *in situ*. The results of this project to date, suggest that this ambitious goal may require some near term compromise. A functionalized gold nanoparticle (Au NP) contrast agent was prepared for biocompatibility, deliverability and damage-specificity. Results have demonstrated damage specificity and a strong binding affinity, especially for alendronate functionalized Au NPs, as well as deliverability. However, these requirements limited the contrast agent to a size and concentration that has only been detected on damaged bone tissue using synchrotron x-ray tomography and not yet been able to be detected on damaged bone tissue using current, commercially available micro-CT technology. Therefore, the results of this work so far suggest that the ambitious goal of non-invasive (*in vivo*) imaging of microdamage in bone would be feasible, *if* new technology were to significantly improve the detection limits and radiation dosage of CT instruments.

On the other hand, an x-ray contrast agent "merely" able to label microdamage in bone (though not biocompatible, deliverable or damage-specific) will still enable non-destructive and three-dimensional (though not *in vivo*) imaging of microdamage in bone. This ability is novel in itself and will provide important new methods for the study of microdamage in bone tissue, as existing methods of damage detection are inherently destructive, two-dimensional and tedious. Results reported in this project are the first to demonstrate and validate these new methods. In light of this, and unless a major breakthough is made, we will continue to investigate Task 3 using the precipitated barium sulfate ($BaSO_4$) stain, which is readily imaged by current, commercially available micro-CT technology.

REFERENCES

1. H. Leng, X. Wang, R.D. Ross, G.L. Niebur and R.K. Roeder, "Micro-computed tomography of fatigue microdamage in cortical bone using a barium sulfate contrast agent," *J. Mech. Behav. Biomed. Mater.*, **1** [1] 68-75 (2008).
2. X. Wang, D.B. Masse, H. Leng, K.P. Hess, R.D. Ross, R.K. Roeder and G.L. Niebur, "Detection of trabecular bone microdamage by micro-computed tomography," *J. Biomechanics*, **40** [15] 3397-3403 (2007).
3. M.D. Landrigan and R.K. Roeder, "Systematic error in mechanical measures of damage during four-point bending fatigue of cortical bone," *J. Biomechanics*, submitted.

APPENDICES

Attached reprints include:

R.D. Ross and R.K. Roeder, "Functionalized Gold Nanoparticle X-ray Contrast Agents for Bone Tissue," *Trans. of the 35th Annual Meeting of the Society for Biomaterials*, San Antonio, TX, **32**, (2009).

M.D. Landrigan, G.L. Niebur and R.K. Roeder, "Detection of Fatigue Microdamage in Human Cortical Bone Using Micro-Computed Tomography," *Trans. of the 55th Annual Meeting of the Orthopaedic Research Society*, Las Vegas, NV, **34**, 2143 (2009).

R.K. Roeder, R.D. Ross and Z. Zhang, "Detection of gold nanoparticles in bone tissue suing x-ray tomography," Proposal GUP-10463, Argonne National Laboratory, submitted July, 2008.

Functionalized Gold Nanoparticle X-ray Contrast Agents for Bone Tissue

Ryan D. Ross[1,2] and Ryan K. Roeder[1,2]
[1]Department of Aerospace and Mechanical Engineering, [2]Bioengineering Graduate Program,
University of Notre Dame, Notre Dame, IN 46556.

Introduction: Repetitive loading of bone tissue can cause damage in the form of microcracks and diffuse damage.[1-3] *In vivo* fatigue microdamage has been shown to correlate with a degradation of mechanical properties including a loss of stiffness and a decrease in fracture toughness, which leads to an increased risk of fracture.[1,3] Current methods for imaging and quantifying microdamage are inherently invasive, destructive and two-dimensional. Therefore, gold nanoparticles (Au NPs) are being investigated as a potential damage-specific X-ray contrast agent due to their biocompatibility, ease of surface functionalization and high X-ray attenuation. Preliminary experiments using glutamic acid functionalized Au NPs showed specificity to damaged regions in bone tissue.[4] The objective of this work was to investigate the effects of different functional groups on specificity and imaging of the contrast agents.

Methods: Au NPs were prepared from $HAuCl_4 \cdot 3H_2O$ (Aldrich) and sodium citrate to a mean particle size of ~ 20 nm using a citrate reduction reaction.[5] Au NPs were then surface functionalized using glutamic acid, 2-aminoethylphosphonic acid or alendronate (Fig. 1). Briefly, 25 mL solution of 0.5 mM Au NP solution was mixed with 1.5 mL 2% poly(vinyl alcohol) (Aldrich, M_w = 50,000-85,000) and 60 mg ion exchange resin (Sigma, Amberlite MB-150) was added to the mixture to remove citrate ions. After stirring overnight, the solution was filtered and 1 mL 0.01 M solution of functional molecule was added. Binding experiments were preformed by adding hydroxyapatite to functionalized Au NP solutions. The suspension was incubated for 4 h to allow for binding and centrifuged. The supernatant solution was collected and the gold concentration was measured using ICP-OES (Perkin-Elmer). Binding constants were derived using a half-reciprocal linearization of Langmuir isotherms. Bovine cortical bone specimens were scratched with a scalpel to induce controlled surface damage and then soaked in a solution of functionalized Au NPs. Specimens were characterized using backscattered scanning electron microscopy (SEM), energy dispersive X-ray analysis (EDXA) and x-ray tomography using a synchrotron light source.

Results: Binding constants of the functionalized Au NPs were 3.82, 0.72 and 0.25 mg/L for alendronate, glutamic acid and phosphonic acid respectively, corresponding to a maximum of 7.33, 1.22 and 0.48 mg Au NPs bound per gram of hydroxyapatite. Thus, alendronate functionalized Au NPs exhibited the highest specificity, as expected, and consequently provided the most visible staining of damaged tissue in backscattered SEM (Fig. 2). Surface damage on similarly prepared specimens labeled with alendronate and glutamic acid functionalized Au NPs was able to be detected using x-ray tomography with a synchrotron light source (Fig. 3).

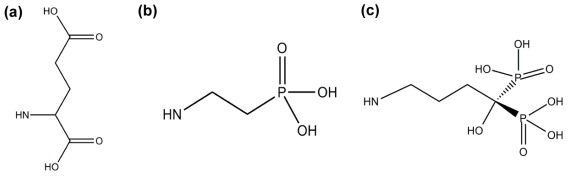

Figure 1. Au NPs were functionalized with (a) glutamic acid (b) 2-aminoethylphosphonic acid or (c) alendronate. Note that each molecule has amino groups for binding on gold surface which are opposite (a) carboxylic acid, (b) phosphonate or (c) bisphosphonate groups for calcium binding in damaged tissue.

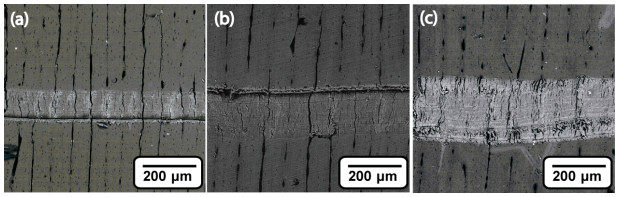

Figure 2. Backscattered SEM micrographs of bovine cortical bone surface damage (scratch) labeled with (a) glutamic acid, (b) phosphonic acid and (c) alendronate functionalized Au NPs, showing enhanced contrast between damaged and non-damaged tissue correlating to the binding affinity of each functional group.

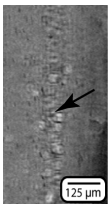

Figure 3. X-ray tomography image of alendronate functionalized Au NP stained bovine cortical bone sample using synchrotron light source, showing enhanced contrast in scratched region (labeled with arrow) corresponding to the presence of Au NPs.

Conclusions: The binding affinity and imaging contrast of functionalized Au NPs was greatest using alendronate followed by glutamic acid and phosphonic acid. Additional binding experiments are being preformed in fetal bovine serum to simulate an *in vivo* environment.

Acknowledgement: USAMRMC W81XWH-06-1-0196 (CDMRP PRMRP PR054672). Use of the Advanced Photon Source was supported by the U. S. Department of Energy, Office of Science, Office of Basic Energy Sciences, under Contract No. W-31-109-Eng-38.

References: [1] AE Tami *et al*,. *J. Orthop. Res.* 21:1018-1024, 2003. [2] R Parkesh *et al*., *Chem. Mater.*,19:1656-1663, 2007. [3] F. O'Brien *et al*., *J. Orthop. Res.*, 23:475-480, 2005. [4] Z Zhang *et al*., *Trans. Soc. Biomats.*, 30:93, 2007. [5] J Turkevich *et al*., *Discuss. Faraday Soc.*, 11:55-75, 1951.

Detection of Fatigue Microdamage in Human Cortical Bone Using Micro-Computed Tomography

[1]Landrigan, M D; [1]+Niebur, G L; [1]+Roeder, R K
+[1]University of Notre Dame, Notre Dame, IN
rroeder@nd.edu

INTRODUCTION:

Conventional techniques used to image microdamage in cortical bone require the preparation of many histologic sections which is inherently invasive, destructive, two-dimensional, and tedious [1]. These limitations inhibit evaluation of the effects of microdamage on whole bone strength and prohibit detection of microdamage *in vivo*. Therefore, micro-computed tomography (micro-CT) has been investigated for the detection of microdamage using iodinated [1], lead sulfide [2,3], and barium sulfate ($BaSO_4$) [4,5] contrast agents. Damage accumulation ahead of a notch in bovine cortical bone beams loaded in cyclic four-point bending was stained *in vitro* by precipitation of $BaSO_4$ and imaged using micro-CT [4]. The objective of this study was to detect the presence and location of fatigue microdamage and/or propagating cracks within a uniformly stressed volume of human cortical bone using micro-CT with a $BaSO_4$ contrast agent.

METHODS:

Twenty specimens were sectioned from the femoral cortex of three adult men (63 ± 1.7 years of age), turned down to a 2.5 mm diameter by 5 mm gauge length using a CNC mini-lathe, and randomly divided into an unloaded control group and loaded group. Specimens were wrapped in gauze, hydrated in PBS, and stored at -20°C in airtight containers during interim periods.

Specimens were tested in load-controlled (R = 0) cyclic uniaxial tension at 2 Hz on an electromagnetic test instrument (Bose Electroforce 3300) while hydrated with a water drip at ambient temperature until a 10% reduction in secant modulus. Specimens were preloaded at 60 MPa for 20 cycles to measure the initial secant modulus and the fatigue load was normalized to an initial maximum strain of 6400 ± 300 microstrain.

Specimens from both groups were stained with $BaSO_4$ by immersion in solutions of equal parts 0.5 M $BaCl_2$, buffered saline, and acetone solution for three days, followed by equal parts 0.5 M $NaSO_4$, buffered saline, and acetone for three days, and rinsed with de-ionized water to remove surface bound particles or ions. The entire gauge length of each specimen was imaged by micro-CT (μCT-80, Scanco Medical) at 10 μm resolution, 70 kVp voltage, 113 μA current, and 200 ms integration time with slices taken perpendicular to the longitudinal axis of the specimen. Images were thresholded to determine the total bone volume (BV) and $BaSO_4$ stained volume (SV).

RESULTS:

Non-specific $BaSO_4$ staining was observed on the free surface and scattered within some Haversian canals in unloaded control specimens (Figs. 1a & 2a). All specimens loaded in cyclic uniaxial tension also exhibited at least one distinct region of concentrated $BaSO_4$ stain which appeared characteristic of fatigue damage and/or propagating cracks (Figs. 1b,c & 2b). The ratio of the thresholded $BaSO_4$ stain volume to bone volume (SV/BV) was significantly greater for the loaded group compared to the control group ($p < 0.05$, t-test) (Fig. 3). There was no correlation between the number of loading cycles and SV/BV ($p = 0.7$).

DISCUSSION:

Micro-CT was able to detect a relatively small volume of fatigue microdamage within a uniformly stressed volume of human cortical bone using a $BaSO_4$ contrast agent. Note that the micro-CT scanner (10 μm resolution) could not detect damage without the use of a contrast agent. In a previous study using similar staining and imaging methods for notched specimens loaded in cyclic four-point bending, distinct regions of bright voxels around the notch tip or along propagating cracks was verified to be due to the presence of precipitated $BaSO_4$ by backscattered electron imaging and energy dispersive spectroscopy [4].

The technique demonstrated in this study is not without limitations. Variability within both experimental groups can be partially attributed to non-specific staining within void space and on free surfaces (Fig. 1). Staining by $BaSO_4$ precipitation is also limited to *in vitro* studies since the staining solutions are not biocompatible.

The specimens in this study will be sectioned and imaged using backscattered SEM to clarify whether the concentrated $BaSO_4$ stain in loaded specimens was due to propagating cracks, accumulated microcracks, and/or diffuse damage. This technique will also be validated against a second loaded group stained and imaged using conventional histological techniques.

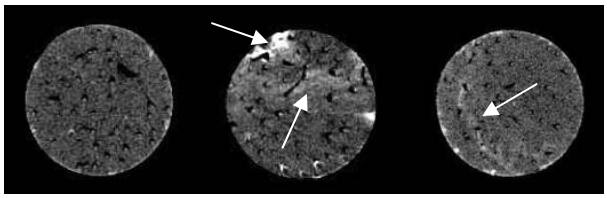

(a) (b) (c)

Fig. 1. Specimen cross-sections (2.5 mm diameter) imaged by micro-CT showing (a) non-specific $BaSO_4$ staining (bright voxels) in unloaded control specimens, and (b,c) regions of concentrated $BaSO_4$ staining in specimens loaded in cyclic uniaxial tension. Arrows highlight regions of $BaSO_4$ staining characteristic of fatigue damage and/or propagating microcracks.

(a) (b)

Fig. 2. Three-dimensional micro-CT reconstructions of the entire gauge section (2.5 mm diameter) in an (a) unloaded control specimen and (b) specimen loaded in cyclic uniaxial tension. Arrows highlight regions of $BaSO_4$ staining characteristic of fatigue damage and/or propagating microcracks.

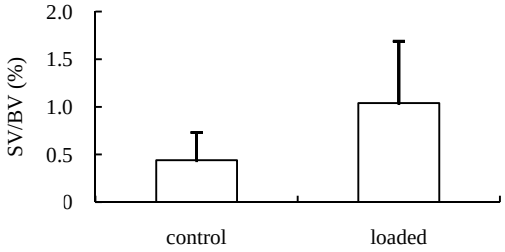

Fig. 3. The ratio of $BaSO_4$ stain volume to total bone volume (SV/BV) in thresholded micro-CT images was significantly greater for the loaded specimens compared to the unloaded control group ($p < 0.05$, t-test). Error bars show one standard deviation.

ACKNOWLEDGEMENTS:

This research was supported by the U.S. Army Medical Research and Materiel Command (W81XWH-06-1-0196) through the Peer Reviewed Medical Research Program (PR054672).

REFERENCES:

1. Lee, *et al.*, *J. Anat*., 203, 161-172 (2003).
2. Leng, *et al.*, *Trans. Orthop. Res. Soc.*, 30, 665 (2005).
3. Tang, *et al.*, *Bone*, 40, 1259-1264 (2007).
4. Leng, *et al.*, *J. Mech. Behav. Biomed. Mater*., 1, 68-75 (2008).
5. Wang, *et al.*, *J. Biomech.*, 40, 3397-3403 (2007).

APS General User Proposal

Proposal Title: Detection of gold nanoparticles in bone tissue using x-ray tomography

GUP Id : 10463

Principal investigator: Ryan Roeder

Proposal Type: Regular Proposal
Status: NEW
Date Submitted:

Subject(s): Materials science, Medical applications, Biological and life sciences, Engineering

Review Panel: Imaging/Microbeam

Required Techniques: Phase contrast imaging, Phase contrast imaging, Tomography, Tomography, Imag

Attached Files:
Reference 1 Leng.pdf
Reference 4 Ross.pdf
None Figure1.pdf

Macromolecular crystallography ? N
Proprietary ? N
Classified ? N
Human subjects / materials ? N
Live animals ? N
Known Safety Hazard ? N

This proposal is related to another General User Proposal
Revision of GUP-8931 which did not make the cut-off for the 2007-3, 2008-1 cycles.

Funding: DOD (specify), CDMRP & PRMRP through the US Army

Scheduling

Total Shifts Requested (Proposal): 6

Scheduling Period: 2008-3
Requested Shifts: 2
Requested Min Shifts: 1

Beamline: First Choice: 13-BM-D-GSECARS
Second Choice: 2-BM-XOR

Scheduling Requirements: As soon as possible. Our samples are prepared and awaiting beam time. A student will commute a three hour drive.

Equipment Requirements: We need x-ray tomography for phase contrast imaging. We will bring no equipment with us.

Unacceptable Dates:

Experimenters

Proposal Progress: Preliminary specimens were sent to Mark Rivers, who attempted some imaging that was unsuccessful in detecting surface damage on cortical bone labeled with gold nanoparticles. Therefore, the experiments in this proposal were designed to overcome the problems encountered with the preliminary specimens and determine the limitations of our approach. Specifically, the proposed experiments will first investigate model specimens comprising variations in known amounts (volume and dimensions) of gold within a bone-like volume. This will enable us to develop working imaging and reconstruction methods, prior to the more challenging specimens of bone microdamage labeled with functionalized gold nanoparticles. Further details are provided in the methods section.

Publications : None. We are a new user. This proposal is for data to include in planned publications.

Name: Ryan Roeder Spokesperson
Institution: University of Notre Dame
Phone: 574-631-7003
E-Mail: rroeder@nd.edu

* Denotes an experimenter who will be on-site at the APS

APS General User Proposal

Name: * Ryan Ross
Institution: University of Notre Dame
Phone: 574-631-1899
E-Mail: rross@nd.edu

Abstract

Proposal Title: Detection of gold nanoparticles in bone tissue using x-ray tomography

Accumulation of microdamage in bone tissue can lead to an increased risk of fracture, including stress fractures in active individuals and fragility fractures in the elderly. Current methods for detecting microdamage are inherently invasive, destructive, tedious and two-dimensional. These limitations inhibit evaluation of the effects of microdamage on whole bone strength and prohibit detection of microdamage in vivo. Therefore, we are investigating novel methods for detecting microdamage in bone using micro-computed tomography (micro-CT) and contrast agents with higher x-ray attenuation than bone. For proof-of-concept, the presence, spatial variation and accumulation of microdamage in cortical and trabecular bone specimens was nondestructively detected by micro-CT using a barium sulfate stain. However, specimens were stained in vitro via a precipitation reaction which was non-specific to damage and not biocompatible. Therefore, we are currently investigating the synthesis and functionalization of gold and barium sulfate nanoparticles for deliverable and damage-specific contrast agents. Unfortunately, commercial micro-CT scanners have been unable to detect the presence of these nanoparticles in damaged bone due to the small size and low concentration. Therefore, the objective of this proposal is to use synchrotron radiation to detect the presence of 1) well-defined volumes of gold deposited via photolithography on a material (aluminum) with similar x-ray attenuation as cortical bone, 2) multiple monolayers of gold nanoparticles deposited on glass slides and 3) surface damage on cortical bone labeled with functionalized gold nanoparticles.

Purpose and importance of research.

Accumulation of microdamage in bone tissue can lead to an increased risk of fracture, including stress fractures in active individuals and fragility fractures in the elderly. Current methods for detecting microdamage are inherently invasive, destructive, tedious and two-dimensional. These limitations inhibit evaluation of the effects of microdamage on whole bone strength and prohibit detection of microdamage in vivo. Therefore, we are investigating novel methods for detecting microdamage in bone using micro-computed tomography (micro-CT) and contrast agents with higher x-ray attenuation than bone. While the phase contrast of a microcrack (water or air) can be detected in bone tissue micro-CT using synchrotron radiation, a damage-specific contrast agent is necessary to distinguish artifactual damage (e.g., due to sample preparation and drying) and specific damage events. Moreover, current commercial and clinical CT instruments are not able to detect microdamage in bone without contrast enhancement due to the small size and low attenuation of microcracks.

For proof-of-concept, the presence, spatial variation and accumulation of microdamage in cortical and trabecular bone specimens was nondestructively detected by micro-CT after staining with barium sulfate [1-3]. However, specimens were stained in vitro via a precipitation reaction which was non-specific to damage and not biocompatible. Therefore, we are currently investigating the synthesis and functionalization of gold and barium sulfate nanoparticles for biocompatible, deliverable and damage-specific contrast agents [4-7]. Functionalized gold nanoparticles have exhibited deliverability via diffusion in bone tissue and specificity for damaged bone tissue [4,5]. Unfortunately, commercial micro-CT scanners have been unable to detect the presence of these nanoparticles in damaged bone due to the small size and low concentration. However, theoretical calculations for the minimum detectable mass fraction of gold in bone tissue suggest feasibility when compared to the surface density of gold nanoparticles on damage bone tissue observed by backscattered SEM [4,8]. Therefore, the objective of this proposal is to use synchrotron radiation to detect the presence of 1) well-defined volumes of gold deposited via photolithography on a material (aluminum) with similar x-ray attenuation as cortical bone, 2) multiple monolayers of gold nanoparticles deposited on glass slides and 3) surface damage on cortical bone labeled with functionalized gold nanoparticles.

Note that this is a highly original research project with significant scientific and clinical implications. There is only one other group in the world (in Ireland) with a comparative level of expertise. Our methods using barium sulfate staining were the first demonstrate non-destructive, three-dimensional detection of microdamage in bone using micro-CT [1-3] and are presently being adopted by other researchers.

Reason for APS.

We have been unable to detect presence of our functionalized gold nanoparticle contrast agent within damaged bone tissue using a commercial micro-CT scanner (Scanco micro-CT 80, 10 μm resolution) due to the necessarily small size and low concentration. The use of synchrotron radiation is expected to provide higher resolution and sensitivity than we have available in our lab. Furthermore, will be able to tune the energy to take advantage of the K-edge for gold, which is not possible with our commercial scanner.

Reason for beamline choice.

Mark Rivers and Francesco DeCarlo have been very helpful with my questions and in facilitating some preliminary measurements.

Previous experience with synchrotron radiation and results.

None. We are a new user. This proposal is for data to include in planned publications.

Description of experiment(s).

Three experiments will be conducted in order to investigate feasibility and demonstrate proof-of-concept:

1) Tomography of well-defined volumes of gold deposited within a material of similar x-ray attenuation to cortical bone tissue. Photolithography has been used to deposit an array of gold islands into acid-etched aluminum (see attached Figure 1). The array consists of square islands ranging in size from 1 to 100 μm, and deposited to a thickness of 0.1 or 1 μm. Aluminum is well-known to exhibit similar x-ray attenuation to cortical bone tissue and is thus used for commercial/clinical x-ray phantoms. Specimen edge effects will be able to be mitigated by "sandwiching" the gold islands against another polished aluminum surface, such that edge detection is aluminum-gold-aluminum without the presence of air. The specimens will be imaged above and below the K-edge for gold at 12 and 11.8 keV. The thickness of the aluminum substrate will be kept less than 1 mm to permit sufficient transmission. Images collected for these specimens will be used to: a) determine the minimum volume or dimension of gold able to be detected with synchrotron radiation vs. a polychromatic commercial micro-CT scanner using the methods employed, b) provide a control specimen and raw image data for the investigation of improved image reconstruction algorithms by a collaborator at Oregon State University (Adel Faridani), and c) develop imaging methods and demonstrate feasibility in a highly controlled model system with a high probability of success before investigating the gold nanoparticles.

2) Radiography and tomography of three, approximately 200 μm x 2 x 20 mm glass slides with a varying number of gold nanoparticle monolayers deposited on one surface. Again, specimen edge effects will be able to be mitigated by "sandwiching" the gold monolayers against another another glass slide, such that edge detection is glass-gold-glass without the presence of air. The specimens will be imaged above and below the K-edge for gold at 12 and 11.8 keV. The glass slides are approximately 500 μm in thickness to permit sufficient transmission. This model system will provide an upper-bound (or near overestimate) for the amount of gold nanoparticles that could be expected to be labeled to a damage surface. To date, we have not been able to detect the presence of these monolayers using our commercial micro-CT.

3) Radiography and tomography of surface damage on bovine cortical bone labeled with functionalized gold nanoparticles [4,5]. Again, specimen edge effects will be able to be mitigated by "sandwiching" the labeled surface damage against another bone specimen, such that edge detection is bone-gold-bone with minimum air gap. The specimens will be imaged above and below the K-edge for gold at 12 and 11.8 keV.

Finally, if unable to detect the gold nanoparticles in experiments 1 and 2 using phase contrast imaging, we would consider forgoing experiment 3 and submitting a new proposal for the use of fluorescence tomography on the specimens from experiments 1 and 2 by collecting two-dimensional image slices.

Estimated amount of beam time, number of visits, number of shifts. (approximately)

Per discussion with Mark Rivers, two 8 hours beam shifts should be sufficient to perform the aforementioned measurements. The two shifts should probably be scheduled at different times, such that data from experiments 1 and 2 can be analyzed prior to exploring experiment 3.

References

1. H. Leng, X. Wang, R.D. Ross, G.L. Niebur and R.K. Roeder, “Micro-computed tomography of fatigue microdamage in cortical bone using a barium sulfate contrast agent,” J. Mech. Behav. Biomed. Mater., 1 [1] 68-75 (2008).
2. X. Wang, D.B. Masse, H. Leng, K.P. Hess, R.D. Ross, R.K. Roeder and G.L. Niebur, “Detection of trabecular bone microdamage by micro-computed tomography,” J. Biomechanics, 40 [15] 3397-3403 (2007).
3. H. Leng, X. Wang, G.L. Niebur and R.K. Roeder, “Fatigue Microdamage in Bovine Cortical Bone Imaged by Micro-Computed Tomography Using a Barium Sulfate Contrast Agent,” Mater. Res. Soc. Symp. Proc., 898E, L09-04 (2005).
4. R.D. Ross, Z. Zhang and R.K. Roeder, “Functionalized Gold Nanoparticles as an X-ray Contrast Agent for Bone Microdamage,” 2008 TMS Annual Meeting, New Orleans, LA (2008). 1st place in the Graduate Division of the Biological Materials Science Symposium Student Poster Contest.
5. Z. Zhang, R.D. Ross and R.K. Roeder, “Functionalized Gold Nanoparticles as a Damage Specific Contrast Agent for Bone,” Trans. of the 33rd Annual Meeting of the Society for Biomaterials, Chicago, IL, 30, 93 (2007).
6. M.J. Meagher, Z. Zhang, and R.K. Roeder, “Precipitation of a Barium Sulfate Nanoparticle Contrast Agent Using Microemulsions,” 2007 TMS Annual Meeting, Orlando, FL (2007).
7. H. Leng, X. Wang, G.L. Niebur and R.K. Roeder, “Synthesis of a Barium Sulfate Nanoparticle Contrast Agent for Micro-Computed Tomography of Bone Microstructure,” Ceram. Trans., 159, 219-229 (2004).
8. K. Kouris, N. M. Spyrou and D. F. Jackson, “Minimum Detectable Quantities of Elements and Compounds in a Biological Matrix,” Nucl. Instrum. Methods, 187, 539-545 (1981).